

Study of multiple degrees of freedom entanglement in optical fiber

Huimin Zhang¹ and Chaoying Zhao^{1, 2, *}

¹*School of Sciences, Hangzhou Dianzi University, Hangzhou 310018, China*

²*State Key Laboratory of Quantum Optics and Quantum Optics Devices, Institute of Opto-Electronics, Shanxi University, Taiyuan 030006, China*

The orbital angular momentum (OAM) has attracted widespread attention due to its ability to carry information in multiple dimensions. However, a high-dimensional entanglement carrying OAM can be affected by environment and undergoes decoherence. Ensuring the stability and high fidelity of entangled states after transmission is a crucial part of quantum communication. How to control the entangled states are essential. In this paper, we produce the polarization entangled photon pairs by type I BBO crystals by means of spontaneous parametric down-conversion (SPDC), we achieve the polarization-OAM hybrid entangled states by *q*-plate (QP) by means of manipulating the multi-degrees of freedom of the quantum state after passing through the APD communication channel. The polarization entangled photon pairs have the characteristics of OAM. We use polarization degree of freedom to modulate OAM degree of freedom, our polarization-OAM hybrid entangled states can slow down the reduction of the fidelity in the during of transmission process. Our quantum states exhibit a superior level of fidelity contrast with the conventional situation. This method will provide a theoretical guidance for improving the transmission fidelity of OAM states in fiber.

Key word:quantum tomography, orbital angular momentum (OAM), fidelity

I. INTRODUCTION

The quantum information technology has led to revolutionary changes in some fields such as communication[1–3], computing and cryptography[4, 5].The concept of fidelity stands as a pivotal yardstick for gauging the quality of quantum information transmission.In the realm of quantum communication, the reliable conveyance of information hinges upon the accurate transmission of quantum states. However, owing to the sensitive characteristics of quantum systems and their susceptibility to environmental noise[6, 7], the practice of channeling quantum states through optical fibers[8, 9], photonic crystal fibers[10], fiber Bragg gratings[11–13], and hollow-core fibers[14] have become prevalent. However, in the transmission process, optical fibers are subject to phase shift[15], dispersion[12, 14] losses and inherent losses, etc. Therefore, how to realize high-capacity quantum state transmission as well as obtaining quantum states with higher fidelity has attract much attention. In the face of these problems, many efforts have been made. Researches have expand the degrees of freedom within quantum states to enhance their information-carrying potential, such as frequency degrees of freedom[16], path degrees of freedom[17], orbital angular momentum (OAM) degrees of freedom[18, 19], and other degrees of freedom[20–23], among which, the OAM degrees of freedom play a huge role in increasing the capacity of quantum states due to their infinite dimensional properties. The establishment of entanglement among diverse degrees of freedom can be realized through four-wave mixing[24], spontaneous parametric down-conversion(SPDC)[25], and the deployment of

quantum memories[26]. Consequently, strategies aimed at preserving the high fidelity of quantum state transmission through optical fibers take on paramount significance. Researches have put forward to using entanglement distillation[27] technology can improve the fidelity of noisy entangled states. Researches also have added the phase to resist the effect of the phase shift generated by the optical fiber to improve the fidelity after transmission[15]. This article aims to delve into the intricate relationship between quantum states and fidelity, while spotlighting the pivotal role quantum states play within optical fiber transmission. we propose a method to modulate the quantum state by modulating the polarization degree of freedom to affect the other degrees of freedom. By methodically manipulating quantum states to optimize fidelity, we embark on a comprehensive exploration that includes discussions on noise channels and the specific intricacies encountered within optical fiber environments. We find that the modulated entangled state can have a better resistance to noise. Our research result can provide a favorable help to guide how to achieve a high-fidelity quantum state transmission.

II. THE MULTIPLE DEGREE OF FREEDOM ENTANGLEMENT GENERATION VIA SPONTANEOUS PARAMETRIC DOWN CONVERSION (SPDC) PROCESSES IN BBO CRYSTAL

A Gaussian pump beam with a wavelength of $\lambda = 1.55\mu m$ goes incident on a polarization beam splitter (PBS) via a mode-matching lens and a high birefringent Beta-Barium Borate (BBO) plate, and then passes through two optical paths including a *q*-plate[8, 28] and two quarter-wave plate (QWP). Here, PBS is used in order to ensure the polarization alignment for maximizing

* zchy49@163.com

the efficiency of phase matching in BBO plate. The entanglement can be manipulated by modulating the optical angle sensor in a digitally enhanced homodyne interferometer in experiments. The measurement sensitivity of the optical angle sensor can be influenced by the BBO plate and the environmental condition. We utilize the spontaneous parametric down-conversion (SPDC) processes to generate signal-idle photon pairs[29–31]. The frequency degree of freedom refer to the frequency difference between the generated signal photons and idle photons, which can be controlled. 0 and 1 can be looked as a quantum representation of the degree of freedom, defining the frequency of one photon as 0 and the other as 1, and forming an entanglement after passing through the SPDC. The OAM degree of freedom can be carried after passing through the q -plate. The reason for putting only one of the two optical paths generated is that the two optical paths are compared and then the effect of the noise channel environment on the photons is compared, as well as the remaining fidelity. The entanglement formed by the upper optical path and the lower optical path is consistent, one of entanglements passes through the APD (amplitude and phase damping) channel, another passes through a single mode fiber(SMF), which can filter the topological charge non-zero photons and purify the polarization entangled photon pairs. We choose the radius of the fiber to be $9.5\mu m$, when the value becomes larger, there are more modes, the coupling becomes more complex, when the value becomes smaller, which may be produce a different modes transfer.

After described the photon pair source generation, we then went further to demonstrate the generation of multiple degrees of freedom entanglement.

Firstly, we carry out a theoretical treatment for the quantification of polarization entanglement for the biphoton state:

$$|\Psi_{pol}\rangle = \alpha|\psi^\dagger(\theta, \phi)\rangle|\psi^\dagger(\theta, \phi)\rangle + \beta|\psi^-(\theta, \phi)\rangle|\psi^-(\theta, \phi)\rangle \quad (1)$$

$$|\psi^\dagger(\theta, \phi)\rangle = \cos\left(\frac{\theta}{2}\right)|0\rangle + e^{i\phi}\sin\left(\frac{\theta}{2}\right)|1\rangle \quad (2)$$

$$|\psi^-(\theta, \phi)\rangle = \sin\left(\frac{\theta}{2}\right)|0\rangle - e^{i\phi}\cos\left(\frac{\theta}{2}\right)|1\rangle \quad (3)$$

which can be continuously varied across a wide range of separable and entangled states, depending on the parameters α and β , and $\alpha^2 + \beta^2 = 1$. The normalized parameter α can be controlled by changing the nonlinear birefringent BBO crystal[30], the value of α maybe obtained by a seventy-two degrees rotation of a QWP in one of the optical paths. θ is the Angle of phase-matching between the pump and the optics axis of BBO crystal. Through the distribution of the phase matching angles, we can obtain the required type of entanglement. ϕ is the phase difference between the two optical path. $|\psi(\theta, \phi)\rangle$ is the state that already select the values of θ and ϕ . The polarization entanglement state takes this form mainly due to the value of θ and ϕ and the form of the state composed of qubits, and the value of θ and $\phi[0, pi]$ is se-

lected because of its periodicity. This value determines the form of entanglement chosen in our paper. $|\psi^\dagger(\theta, \phi)\rangle$ and $|\psi^-(\theta, \phi)\rangle$ are the expressions of arbitrary basis of a single qubit (we use the superscript '+' and '-' to distinguish the different basis). The probabilities of the entangled states generated through the SPDC process is $\cos(\theta/2)$ and $\sin(\theta/2)$, respectively.

Secondly, the initial Guassian state defined as $|0\rangle$ in order to more conveniently describe the change of photons after passing through the device, and the subsequent $|0\rangle$ and $|1\rangle$ represents the OAM entangled state with topological charge $l = 1$ and $l = -1$, respectively. The entangled state comprises two photons. We neglect the fundamental mode, the OAM entangled states $l = 1$ and $l = -1$ are analogous to the cases of logical 0 and 1, respectively. Let's consider the evolution of a single photon as follows:

$$|0\rangle|H\rangle \xrightarrow{QWP} |0\rangle|R\rangle \xrightarrow[q=l/2]{q-plate} |l\rangle|L\rangle \xrightarrow{QWP} |l\rangle|H\rangle \quad (4)$$

$$|0\rangle|V\rangle \xrightarrow{QWP} |0\rangle|L\rangle \xrightarrow[q=l/2]{q-plate} |-l\rangle|R\rangle \xrightarrow{QWP} |-l\rangle|V\rangle \quad (5)$$

where $|L\rangle$ represents the left-handed circularly polarized light, and $|R\rangle$ represents the right-handed circularly polarized light. The q -plate has a order of $l/2$, and the generated OAM light with the topology change l . This allowed us to transform the initial polarization entangled state $|\Psi_{pol}\rangle$ into the state $|\Psi\rangle$.

Thirdly, a quantum system is often affected by an external environment, the dissipation is a irreversible process, which will result in a decoherence phenomenon. We will adopt the amplitude and dephase channel method[6] for simulating the decoherence process. In this paper, we set entangled beams passing through a hybrid noise channel optical fiber, which composed of the amplitude damping (AD) noise channel and the phase damping (PD) noise channel. We take the proportions of both the AD noise channels and the PD noise channels 50%, namely the influence of the two noise channels is evenly balanced. T_1 is the relaxation time of the AD noise channel, t_1 is the transmission time through the AD noise channel. T_2 is the dephasing time of the PD noise channel[6], and t_2 is the transmission time through the PD noise channel. The static noise channel need consider dispersion, a low aberration coefficient (1%) will make the dispersion becomes small, so the effect of dispersion should not be considered. We set $t_1 = t_2 = 100\mu s$ [6], we can see the advantages under this condition more clearly. When the amplitude and dephase damping noise acts on any arbitrary quantum state ρ , there is a certain probability of inverting qubits[6], $\varepsilon(\rho) = |\psi\rangle\langle\psi|$ denotes the quantum states unaffected by noise. Therefore, the Krause operators E_0 , E_1 , E_2 in the APD noise channel have the

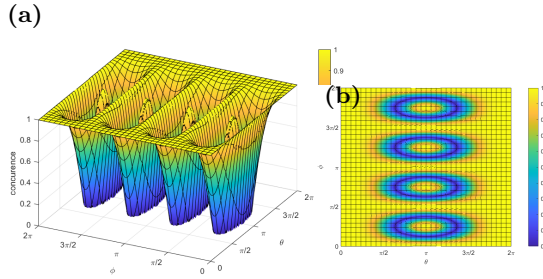


Fig 1. (a) Variation of a concurrence parameter ($C(\Psi)$) with the Angle of phase-matching (θ) and the phase difference (ϕ) in 3-D plot. The maximum value of $C(\Psi)$ ($C(\Psi) = 1$) can be attained when $\theta = n\pi/4$, $\phi = \pi$. (b) The projection of (a) on θ and ϕ two dimensional images.

following relationships:

$$\rho = |\Psi\rangle\langle\Psi| \quad (6)$$

$$\varepsilon(\rho) = \sum_{m,n=0}^2 \hat{E}_m \otimes \hat{E}_n |\Psi\rangle\langle\Psi| \otimes \hat{E}_m^\dagger \otimes \hat{E}_n^\dagger \quad (7)$$

$$E_0 = \begin{bmatrix} 1 & 0 \\ 0 & \sqrt{1 - \gamma_d - (1 - \gamma_d)\gamma_s} \end{bmatrix} \quad (8)$$

$$E_1 = \begin{bmatrix} 0 & \sqrt{\gamma_d} \\ 0 & 0 \end{bmatrix} \quad (9)$$

$$E_2 = \begin{bmatrix} 0 & 0 \\ 0 & \sqrt{(1 - \gamma_d)\gamma_s} \end{bmatrix} \quad (10)$$

where γ_d represents the damping noise and γ_s represents the scattering noise.

Lastly, there are various measure methods were proposed in order to quantify the entanglement, the most famous is concurrence. With the help of quantum state tomography, concurrence can reconstitute a high-dimensional entanglement[32]. In this paper, we can calculate concurrence of any pure state Ψ by using the following relations:

$$C(\Psi) = |\langle\psi|\tilde{\psi}\rangle|^2 \quad (11)$$

$$|\tilde{\psi}\rangle = \sigma_y^{\otimes n}|\psi\rangle \quad (12)$$

where σ_y is the Pauli matrix, and n represents the number of qubits. For the sake of computational convenience, with the increasing of θ and ϕ , the concurrence maintains a noise-free situation(see Fig.1). When we choice $\phi = \pi$, $t = 0$, we find that $\alpha = 1/\sqrt{2} = 0.707$ is the noise-free situation. If we consider the influence of noise, α is no longer a value of constant, but different values of changes over time. We demonstrate the changes in fidelity and concurrence under different values of α .(see Fig.3). When θ changes over time, by numerical simulating, we find that $\alpha \in (0.65, 0.8)$ states can get a better

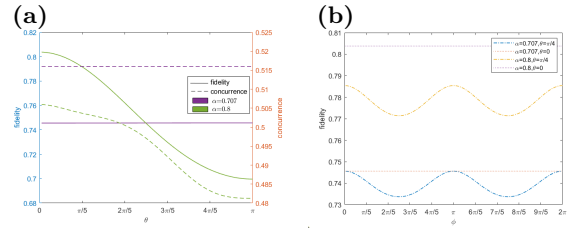


Fig 2. (a) Variation of fidelity and concurrence with θ , the purple solid line corresponds to $\alpha = 0.707$ and the green solid line corresponds to $\alpha = 0.8$. (b) Variation of fidelity with ϕ . The solid line represents $\theta = 0$ case. The dashed line represents $\theta = \pi/4$ case. When $\theta = 0, \pi/4$, the concurrence and fidelity are better than that of the $\theta = \pi/2, \pi$ situation

results from Fig.3(a). Form Fig.2(a), the value of $\theta = \pi$ is relatively small, therefore, we need not take into account this situation. In the following calculations, firstly, we choose $\alpha = 0.65, 0.707, 0.8$, respectively. By comparing the conclusions of Fig.3(c)-3(d), we can easily find that $\theta = 0, \alpha = 0.8$ state can yields a longer survival time and a higher fidelity and concurrence with the time increasing. Secondly, we continue to investigate ϕ changes over time when given $\theta = 0, \alpha = 0.8$. Referring to Fig.2(b), we find that the values of ϕ have no impact on the overall outcome. However, it is still necessary to consider the impact of ϕ on the overall outcome when $\theta \neq 0, \alpha = 0.8$. Thus, the output states from the entangled qubits are:

$$|\Psi_{final}\rangle = 0.8|HH\rangle \otimes |l,l\rangle + 0.6|VV\rangle \otimes |-l,-l\rangle \quad (13)$$

The scenarios described above did not account for the entanglement between frequencies that accompanies the process of SPDC-generated entanglement. Therefore, the subsequent discussion will focus on the frequency degree of freedom.

$$|\Psi\rangle = |\Psi_{final}\rangle \otimes |\Psi_{fre}\rangle \quad (14)$$

$$|\Psi_{fre}\rangle = |10\rangle + |01\rangle \quad (15)$$

Upon introducing the frequency degree of freedom, the overall trend of the states remains consistent with the previous scenario in the absence of noise. Therefore, we continue to use the same values of θ and ϕ as 4 qubits case, thus, we can determine the range of value of α .

In this paper, the situation that the fidelity in the case of $t = 10\mu\text{s}$ for 6 qubits in the noise channel like the situation that the fidelity can reaches to 0.71 after transmission of 1km for distribution [15], which use both OAM and frequency entanglement. If we set the propagation speed in optical fiber equal to 0.2ns/m , the transmission distance should be 2km . The transmission distance is converted to $t = 5$, if adopt our method, fidelity will be higher. For 6 qubits cases, we consider three degrees of freedom, including polarization, frequency, and OAM, whereas the OAM degree of freedom can realize a high-dimensional entanglement, the polarization degree

Table.1 The improvement of fidelity between $\alpha = 0.8$ and $\alpha = 0.707$.

	time/ μ s	10	30	50	80	100
4 – qubits	$\alpha = 0.707$	0.7456	0.4557	0.3682	0.3109	0.3016
	$\alpha = 0.8$	0.8038	0.5997	0.5149	0.4647	0.4549
	Fidelity improve ratio	7.81%	31.60%	39.84%	49.47%	50.83%
6 – qubits	$\alpha = 0.707$	0.6347	0.2876	0.1601	0.0976	0.0769
	$\alpha = 0.8$	0.6843	0.3626	0.2291	0.1439	0.116
	Fidelity improve ratio	7.81%	26.08%	43.10%	47.44%	50.85%

Table.2 The improvement of fidelity between $\alpha = 0.8$ and $\alpha = 0.707$ with different l .

	time/ μ s	10	30	50	80	100	200	300
$l=4$	$\alpha = 0.707$	0.8806	0.6828	0.5552	0.4507	0.4123	0.3327	0.2913
	$\alpha = 0.8$	0.8956	0.7177	0.5988	0.498	0.4598	0.3773	0.3342
	Fidelity improve ratio	1.70%	5.11%	7.85%	10.49%	11.52%	13.41%	14.73%
$l=8$	$\alpha = 0.707$	0.8351	0.5819	0.4335	0.3218	0.2831	0.2071	0.1709
	$\alpha = 0.8$	0.8493	0.6117	0.4675	0.3555	0.3157	0.2349	0.1961
	Fidelity improve ratio	1.70%	5.12%	7.84%	10.47%	11.52%	13.42%	14.75%
$l=16$	$\alpha = 0.707$	0.7919	0.4959	0.3384	0.2297	0.1944	0.129	0.1003
	$\alpha = 0.8$	0.8054	0.5213	0.365	0.2598	0.2167	0.1463	0.115
	Fidelity improve ratio	1.70%	5.12%	7.86%	13.10%	11.47%	13.41%	14.66%

of freedom serves mainly to modulate the quantum state. Due to the linear polarization direction in actually fiber will changes with the azimuthal angle of the change [33], which will lead to a instability in transmission process. Therefore, we should convert the linear polarization into circular polarization before put it into the optical fiber, and the circular polarization and the OAM degrees of freedom can form a stable OAM mode.

The inclusion of the frequency degree of freedom is reflected in Fig.(4(a)) graph, where the range of value of α has transitions from (0.65-0.8) to (0.7-0.9), undergone a tiny right shifts. Consequently, in the case of 6 qubits, we set $\alpha = 0.9$. However, upon closer examination (of see Fig.(4(d))) we note that $\alpha = 0.9$ has a higher fidelity over time compared to another two cases. However, $\alpha = 0.9$ has a notably low-lying initial entanglement levels, so $\alpha = 0.9$ isn't a favorable choice. Considering both Fig.(4) and Fig.(6), $\alpha = 0.8$ is an optimal value. OAM mentioned above are solely considering the individual state $|l\rangle$, without taking all these states into account such as $|l-1\rangle, \dots, |1\rangle$. For example, if we take $l = 4$, we should take into account $|4\rangle, |3\rangle, |2\rangle$ and $|1\rangle$ at the same time[38]. Therefore, it's necessary to discuss the OAM degree of freedom entanglement. Fig.5 unmistakably illustrates that the Fidelity of $\alpha = 0.8$ consistently surpasses that of $\alpha = 0.707$ case.

We give out a preliminary estimate of the value of α is 0.8, but it is not an optimal value in the presence of noise. The ideal value of α will varies depending on dif-

ferent actual conditions. Nevertheless, α with an approximate range of 0.8, which tends to improve the Fidelity of entanglement. Next, Fibre transport of the spatially entangled 4 qubits through the optical fibers and examine whether the value of α is applicable to our situation.

III. ENTANGLEMENT EVOLUTION IN OPTICAL FIBER IN THE PRESENCE OF NOISE

We find that the linear polarization direction will changes with the azimuthal Angle[33], the optical characteristics of the linearly polarized modes in optical fiber will result in an instability problem, we contemplate on a QWP in order to transforming the linearly polarized mode into a circularly polarized mode before entering the optical fiber. The circularly polarized mode with the OAM degrees of freedom can form a stable OAM mode. The prepared enantagled state may be affected by various factors such as dispersion[12], and noise[39]. Therefore, the entangled state in the optical fiber can be expressed

Table.3 Comparison of seven schemes.

	Entanglement type	Environmental	Modulation method	Conversion Efficiency	Fidelity
2015[34]	Polarization	-	-	-	99%
2018[35]	Polarization-OAM	-	-	-	70.8%
2018[36]	OAM	-	SLM(phase)	-	85.81%
2020[15]	OAM	fiber(1km)	SLM(phase)	-	71%
2020[27]	Polarization-OAM	AD channel ^a	Distillation	-	60% ^b
2021[37]	SAM-OAM	-	fiber	90%	-
Our work	Polarization-OAM	APD Channel ^c (2km ^d)	QWP	-	80.38%
	Polarization-OAM	APD Channel(2km ^e)	QWP	-	68.43%

^a Amplitude Damping Channel

^b we choose Two-photons case, and $T_1=T_2$, $\lambda = 0.8$.

^c Amplitude and Phase Damping Channel

^d we selected 4 qubits cases and $t = 10\mu s$, consider the speed of light as $0.2ns/m$.

^e we selected 6 qubits cases and $t = 10\mu s$, consider the speed of light as $0.2ns/m$.

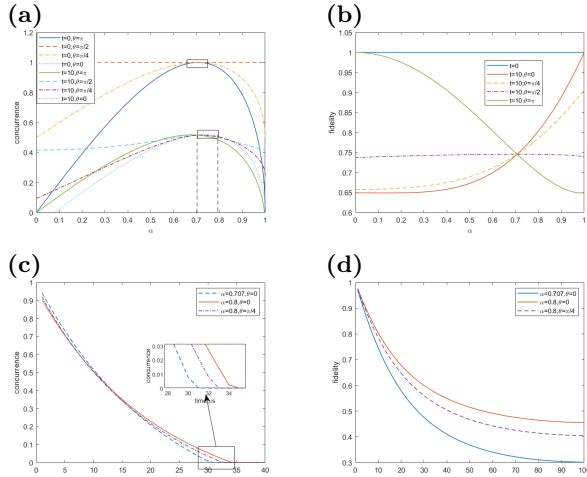


Fig 3. 4 qubits hybrid entangled when $\phi = \pi$. (a) Variation of concurrence with α . (b) Variation of fidelity with α . The relationship between "concurrence and fidelity" and variation of α with θ Angles. The region enclosed within the boxed area represents the range of select-able "concurrence" values (without considering $\theta = \pi$ case). (c) Variations of concurrence with t . (d) Variations of fidelity with t under different α and θ Angles.

as [37]:

$$\hat{U}_{fiber} = \int f(\omega_s, \omega_i) e^{i\beta_{fiber}z} dr \quad (16)$$

$$\beta_{fiber} = \frac{2\pi n_{eff}}{\lambda_{photon}} \quad (17)$$

$$\begin{aligned} |\Psi_{fiber}\rangle &= \hat{U}_{fiber} |\Psi_{in}\rangle \\ &= \int f(\omega_s, \omega_i) d\omega_s d\omega_i (0.8e^{i\beta_1 z}|1,1\rangle \\ &\quad + 0.6e^{i\beta_2 z}| -1, -1\rangle) \otimes |\Psi_{fre}\rangle \end{aligned} \quad (18)$$

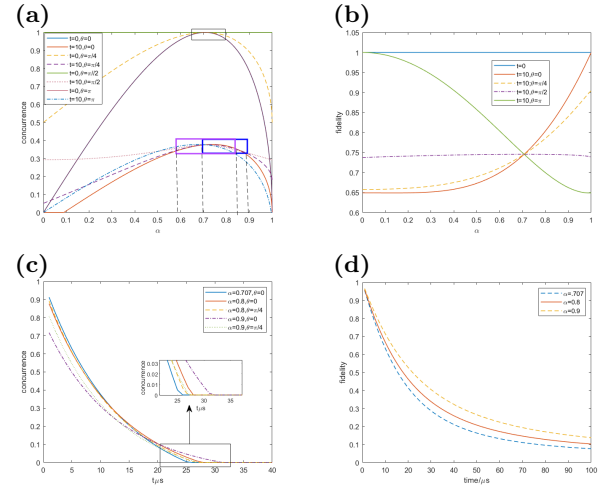


Fig 4. 6 qubits hyper-entangled when $\phi = \pi$. (a) Variation of concurrence with α . The lower left region is the vortex area of $\theta=\pi/2$ and $\theta=\pi$, while the lower-right region corresponds to the vortex area of $\theta=\pi/4$ and $\theta=0$. (b) Variation of fidelity with α . (c) Variation of concurrence with α . (d) Variation of fidelity with α .

where $\alpha = 0.8$, $\beta = 0.6$. z is the transmission distance in hybrid channel. The topological changes l of OAM depends on the order of the q -plate and the circularly polarized state. $| -1, -1\rangle$ state generated by q -plate. $|\Psi_{in}\rangle$ is the initial state prepared outside the fiber, we set $m = 1$, and the evolution operator \hat{U}_{fiber} represents the influence of the fiber on the state. where β is the propagation constant in the optical fiber, while n_{eff} is the effective refractive index within the fiber. Typically, these values are associated with the optical fiber mode, OAM topology, and frequency, β_1 is the propagation constant when topology $l = 1$, and β_2 is the propagation constant when topology $l = 2$. z is the transmission dis-

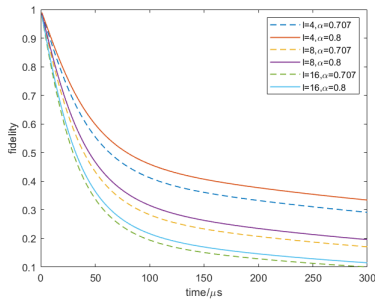


Fig 5. Variation of fidelity with topological charge l and α . The red solid line, the purple solid line and the blue solid line corresponds to $\alpha = 0.8$ and $l = 4, 8, 16$, respectively. The blue dashed line, the orange dashed line and the green dashed line corresponds to $\alpha = 0.707$ and $l = 4, 8, 16$, respectively.

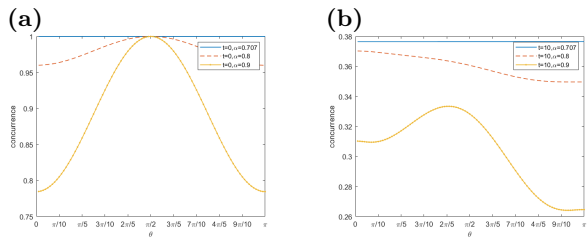


Fig 6. Variation of concurrence with α and t . (a) Variation of concurrence under noiseless conditions when $t = 0$. (b) Variation of concurrence with θ when $t = 10$.

tance in the fiber, λ_{photon} is the wavelength of photon. ω_s and ω_i is the frequency of signal and idle photon, respectively, $f(\omega_s, \omega_i)d\omega_s d\omega_i$ represents the radial distribution function, and $\int |f(\omega_s, \omega_i)|^2 d\omega_s d\omega_i = 1$.

We discuss hyper-entangled photon pairs in optical fibers[23], we calculate the tensor product of SAM and OAM degrees of freedom, which are generated directly through SPDC process. We can derived out the CHSH inequality (except the frequency DOF) by projecting the entanglement into sub-spaces, where \hat{P} is the project op-

erator, X , Y and Z are the Pauli matrices.

$$\begin{aligned}
 |h_1\rangle &= (|H\rangle + |v\rangle)/\sqrt{2}, |v_1\rangle = (|H\rangle - |v\rangle)/\sqrt{2} \quad (19) \\
 |h_2\rangle &= (|m\rangle + |-m\rangle)/\sqrt{2}, |v_2\rangle = (|m\rangle - |-m\rangle)/\sqrt{2} \\
 \hat{P}_1 &= |h_1 h_1\rangle \langle h_1 h_1| \\
 &= (|HH\rangle + |VV\rangle + |HV\rangle + |VH\rangle) \\
 &\quad (\langle HH| + \langle VV| + \langle HV| + \langle VH|)/4 \\
 &= (|HH\rangle + |VV\rangle + |HV\rangle + |VH\rangle)(\langle HH| + \langle VV|)/4 + \dots \\
 \hat{P}_2 &= |v_1 v_1\rangle \langle v_1 v_1|, \hat{P}_3 = |h_2 h_2\rangle \langle h_2 h_2| \\
 \hat{P}_4 &= |v_2 v_2\rangle \langle v_2 v_2|, |\psi_p\rangle = \hat{P}|\Psi_{\text{final}}\rangle \\
 \hat{A}_1 &= (X + Z)/\sqrt{2}, \hat{A}_2 = (X - Z)/\sqrt{2} \\
 \hat{B}_1 &= X, \hat{B}_2 = Z \\
 \hat{a}_1 &= (X + Y)/\sqrt{2}, \hat{a}_2 = (X - Y)/\sqrt{2} \\
 \hat{b}_1 &= X, \hat{b}_2 = Y \\
 \langle \hat{A} \hat{B} \rangle &= \langle \psi_p | \hat{A} \hat{B} | \psi_p \rangle \\
 CHSH_{\text{pol}} &= \langle \hat{A}_1 \hat{B}_1 \rangle + \langle \hat{A}_1 \hat{B}_2 \rangle + \langle \hat{A}_2 \hat{B}_1 \rangle - \langle \hat{A}_2 \hat{B}_2 \rangle \\
 CHSH_{\text{OAM}} &= \langle a_1 b_1 \rangle + \langle a_1 b_2 \rangle + \langle a_2 b_1 \rangle - \langle a_2 b_2 \rangle \\
 X &= \begin{bmatrix} 0 & 1 \\ 1 & 0 \end{bmatrix} Y = \begin{bmatrix} 0 & -i \\ i & 0 \end{bmatrix} Z = \begin{bmatrix} 1 & 0 \\ 0 & -1 \end{bmatrix}
 \end{aligned}$$

By calculation, we can get the different project operations, \hat{P}_1 and \hat{P}_2 are the same, \hat{P}_3 and \hat{P}_4 are the same, and $CHSH_{\text{pol}}=2.8284$, it is the Maximum entanglement, $CHSH_{\text{OAM}}=2.7153$, it is not the Maximum entanglement due to the SAM entanglement with a coefficient.

In this paper, we adopt standard single-mode fiber[15]. In addition to the calculation of quantum noise mentioned above, we must consider the whole intrinsic fiber loss such as the absorption loss, the dispersion loss and the scattering loss caused by the fiber structural defects. In the following calculation, we take the whole intrinsic fiber loss equal to $0.36 \text{ dB}/\text{km}$ [40]. Understanding the transmission process is crucial for investigate the evolution of entanglement, we introduce phase shifts factors when topological charge $l = 1$ ($\theta_1 = 1.02\pi$, $\phi_1 = 0.98\pi$ [15]). Based on the effective refractive index n_{neff} in the optical fiber, we find that between propagation mode $m = 1$ and propagation mode $m = -1$ indication of a substantial degeneracy[41]. Hence, we select the value of $n_1 = n_{-1} = 1.448$ [15]. The pump wavelength $\lambda_{\text{pump}} = 1550\text{nm}$. We investigate the fidelity changes with the transmission distance.(see Fig.7). From the two dotted boxes in Fig.7 we find that the Fidelity curves has a clear oscillation with stable periodic characteristics. Previous studies have reported that researcher can convert periodically spin angular momentum (SAM) to OAM in weakly-coupled few-mode fibers[37], if we furthermore convert this result to the fidelity, which is in agreement with periodic characteristic. The entire state

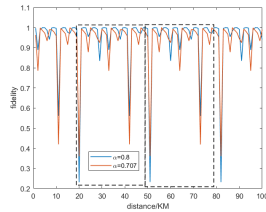


Fig 7. Variation of fidelity with transmission distance

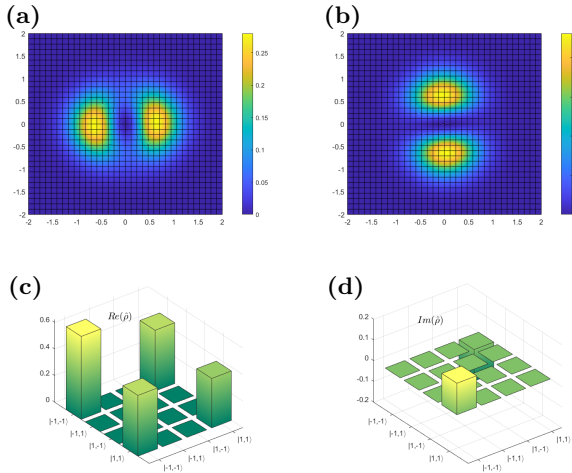


Fig 8. The intensity distribution of the light beam after the first(a) and second(b) projections. (c) and (d) represents the real and imaginary parts of the OAM condition after reconstruction, respectively.

fidelity is

$$|\Psi_{fiber}\rangle = \int f(\omega_s, \omega_i) d\omega_s d\omega_i (0.8e^{i\beta_1 z} e^{i\theta_1} |1, 1\rangle + 0.6e^{i\beta_2 z} e^{i\phi_1} | -1, -1\rangle) \otimes |\Psi_{fre}\rangle \quad (20)$$

It is evident from Fig.(7) that there isn't a substantial disparity between $\alpha = 0.707$ and $\alpha = 0.8$ at the peaks values of the Fidelity. Nevertheless, the distinct advantage lies in the fact that $\alpha = 0.8$ has a broader range of favorable positions in comparison to that of $\alpha = 0.707$ case. Subsequently, we shift the focus to examining the impact of optical fiber on the OAM degree of freedom after transmission has been completed. For this purpose,

we use the two-measurement tomography method[42] to reconstruct the output beam when $z = 95\text{km}$. We can observe the changes in the OAM degree of freedom before and after the output. In the OAM scenario, we can calculate that the fidelity after the reconstruction reaches around 98% compared to that of before the incident beam. Considering Figs.7-8, the quantum bit configuration also performs well in the optical fiber. But the situation of quantum distribution is not discussed in this paper, and we will study it in our future work.

IV. CONCLUSION

In this paper, we propose a method of quantum state modulation that allows us to obtain quantum states with higher fidelity in different situations. We consider the performance in optical fibers and find that the tuned quantum states exhibit better stability, in which high fidelity can be achieved at $\alpha = 0.8$, which ensures that our tuned states can be transported with better stability and a wider range. We develop the discussion in the APD (amplitude and phase damping) channel as well as in the fiber condition. The results show that the tuned entangled state in the APD channel performs the regular state to a certain extent, and its corresponding fidelity improves by 7% at $10\mu\text{s}$, both for the 4 qubits case and the 6 qubits case, with the advantage becoming more pronounced with increasing time. The fidelity improvement is also more significant when considering only the OAM entangled state, which at $100\mu\text{s}$ improves the fidelity by about 10%. Compared with the conventional situation, our entangled states can generate a better fidelity and obtain a better stability. The main scope of our work is to improve the transmission fidelity of OAM states in fiber.

Author contributions: H. Zhang performed the simulation, supervised by C. Zhao. H. Zhang and C. Zhao prepared the manuscript. C. Zhao supervised the project.

Disclosures

Others declare no conflicts of interest.

Data Availability Statement

Data and simulation codes related to this work are available from the corresponding author upon reasonable request.

[1] Tara Fortier and Esther Baumann. 20 years of developments in optical frequency comb technology and applications. *Communications Physics*, 2, December 2019.
[2] Peiying Zhang, Ning Chen, Shigen Shen, Shui Yu, Sheng Wu, and Neeraj Kumar. Future quantum communications and networking: A review and vision. *IEEE Wireless Communications*, 2022.
[3] Daniele Cozzolino, Beatrice Da Lio, Davide Bacco, and

Leif Katsuo Oxenløwe. High-dimensional quantum communication: Benefits, progress, and future challenges. *Advanced Quantum Technologies*, 2(12):1900038, 2019.
[4] Lai Zhou, Jinping Lin, YuanMei Xie, YuShuo Lu, Yumang Jing, HuaLei Yin, and ZhiLiang Yuan. Experimental quantum communication overcomes the rate-loss limit without global phase tracking. *Physical Review Letters*, 130(25):250801, June 2023.

[5] YiChen Zhang, Ziyang Chen, Stefano Pirandola, Xiangyu Wang, Chao Zhou, Binjie Chu, Yijia Zhao, Bingjie Xu, Song Yu, and Hong Guo. Long-distance continuous-variable quantum key distribution over 202.81 km of fiber. *Physical Review Letters*, 125(1):010502, June 2020.

[6] Josu Etxezarreta Martinez, Patricio Fuentes, Pedro Crespo, and Javier Garcia-Frias. Time-varying quantum channel models for superconducting qubits. *npj Quantum Information*, 7(1), July 2021.

[7] Rajiuddin Sk and Prasanta K. Panigrahi. Protecting quantum coherence and entanglement in a correlated environment. *Physica A: Statistical Mechanics and its Applications*, 596:127129, June 2022.

[8] Junyi Liu, Jingxing Zhang, Jie Liu, Zhenrui Lin, Zhenhua Li, Zhongzheng Lin, Junwei Zhang, Cong Huang, Shuqi Mo, Lei Shen, Shuqing Lin, Yujie Chen, Ran Gao, Lei Zhang, Xiaobo Lan, Xinlun Cai, Zhaohui Li, and Siyuan Yu. 1-pbps orbital angular momentum fibre-optic transmission. *Light: Science & Applications*, 11(1):202, 2022.

[9] Junyi Liu, Zhenrui Lin, He Zhu, Lei Shen, Shuqi Mo, Zhenhua Li, Jingxing Zhang, Junwei Zhang, Xiaobo Lan, Jie Liu, and Siyuan Yu. 1120-channel OAM-MDM-WDM transmission over a 100-km single-span ring-core fiber using low-complexity 4×4 MIMO equalization. *Optics Express*, 30(11):18199–18207, 2022.

[10] Haihao Fu, Chao Liu, Zao Yi, Xinpeng Song, Xianli Li, Yanshu Zeng, Jianxin Wang, Jingwei Lv, Lin Yang, and Paul K. Chu. A new technique to optimize the properties of photonic crystal fibers supporting transmission of multiple orbital angular momentum modes. *Journal of Optics*, 52(1):307–316, March 2023.

[11] Hang Wu, Shecheng Gao, Bingsen Huang, Yuanhua Feng, Xincheng Huang, Weiping Liu, and Zhaohui Li. All-fiber second-order optical vortex generation based on strong modulated long-period grating in a four-mode fiber. *Optics Letters*, 42(24):5210–5213, December 2017.

[12] Fathy M. Mustafa, Hisham A. Kholidy, Ahmed F. Sayed, and Moustafa H. Aly. Enhanced dispersion reduction using apodized uniform fiber bragg grating for optical mtmdm transmission systems. *Optical and Quantum Electronics*, 55, December 2023.

[13] Laipeng Shao, Shen Liu, Min Zhou, Min Zhou, Zheng Huang, Weijia Bao, Zhiyong Bai, Zhao Liu, Guoxuan Zhu, Zhongyuan Sun, Junlan Zhong, and Yiping Wang. High-order OAM mode generation in a helical long-period fiber grating inscribed by an oxyhydrogen-flame. *Optics Express*, 29(26):43371–43378, 2021.

[14] Wenqian Zhao, Wenpu Geng, Yingning Wang, Yuxi Fang, Changjing Bao, Yongxiong Ren, Weigang Zhang, Hao Zhang, Zhongqi Pan, and Yang Yue. Air-core non-zero dispersion-shifted fiber with high-index ring for OAM mode. *IEEE Access*, 9:107804–107811, 2021.

[15] Huan Cao, She-Cheng Gao, Chao Zhang, Jian Wang, De-Yong He, BiHeng Liu, ZhengWei Zhou, YuJie Chen, ZhaoHui Li, Si-Yuan Yu, Jacqueline Romero, YunFeng Huang, ChuanFeng Li, and GuangCan Guo. Distribution of high-dimensional orbital angular momentum entanglement over a 1 km few-mode fiber. *Optica*, 7(3):232–237, 2020.

[16] Manuel Erhard, Mario Krenn, and Anton Zeilinger. Advances in high-dimensional quantum entanglement. *Nature Reviews Physics*, 2(7):365–381, 2020.

[17] XiaoMin Hu, WenBo Xing, BiHeng Liu, YunFeng Huang, ChuanFeng Li, GuangCan Guo, Paul Erker, and Marcus Huber. Efficient generation of high dimensional entanglement through multipath down conversion. *Physical Review Letters*, 125(9):090503, 2020.

[18] LingJun Kong, Yongnan Li, Rui Liu, WenRong Qi, Qiang Wang, ZhouXiang Wang, ShuangYin Huang, Yu Si, Chenghou Tu, Wei Hu, Fei Xu, YanQing Lu, and HuiTian Wang. Complete measurement and multiplexing of orbital angular momentum bell states. *Physical Review A*, 100(2):023822, 2019.

[19] Long Zhu, Andong Wang, Shi Chen, Jun Liu, Qi Mo, Cheng Du, and Jian Wang. Orbital angular momentum mode groups multiplexing transmission over 2.6-km conventional multi-mode fiber. *Optics Express*, 25(21):25637–25645, 2017.

[20] S. P. Walborn, S. Pádua, and C. H. Monken. Hyperentanglement assisted bell state analysis. *Physical Review A*, 68(4):042313, 2003.

[21] GuanYu Wang, Qian Liu, and Fu-Guo Deng. Hyperentanglement purification for two-photon six-qubit quantum systems. *Physical Review A*, 94(3):032319, 2016.

[22] TianMing Zhao, Yong Sup Ihn, and YoonHo Kim. Direct generation of narrow-band hyperentangled photons. *Physical Review Letters*, 122(12):123607, 2019.

[23] Julio T. Barreiro, Nathan K. Langford, Nicholas A. Peters, and Paul G. Kwiat. Generation of hyperentangled photon pairs. *Physical Review Letters*, 95(26):260501, 2005.

[24] LanTian Feng, Ming Zhang, Xiao Xiong, Yang Chen, Hao Wu, Ming Li, GuoPing Guo, GuangCan Guo, DaoXin Dai, and XiFeng Ren. On-chip transverse-mode entangled photon pair source. *npj Quantum Information*, 5(1):1–7, January 2019.

[25] Zichang Zhang, Chenzhi Yuan, Si Shen, Hao Yu, Ruiming Zhang, Heqing Wang, Hao Li, You Wang, Guangwei Deng, Zhiming Wang, Lixing You, Zhen Wang, Haizhi Song, Guangcan Guo, and Qiang Zhou. High-performance quantum entanglement generation via cascaded second-order nonlinear processes. *npj Quantum Information*, 7(1):1–9, August 2021.

[26] Wei Zhang, DongSheng Ding, MingXin Dong, Shuai Shi, Kai Wang, ShiLong Liu, Yan Li, ZhiYuan Zhou, BaoSen Shi, and GuangCan Guo. Experimental realization of entanglement in multiple degrees of freedom between two quantum memories. *Nature Communications*, 7(1):13514, November 2016.

[27] Dan-Yang Chen, Zhi Lin, Ming Yang, Qing Yang, Xue-Ping Zang, and Zhuo-Liang Cao. Distillation of lossy hyperentangled states. *Physical Review A*, 102(2):022425, August 2020.

[28] Yudong Lian, Xuan Qi, Yuhe Wang, Zhenxu Bai, Yulei Wang, and Zhiwei Lu. Oam beam generation in space and its applications: A review. *Optics and Lasers in Engineering*, 151:106923, April 2022.

[29] S. Magnitskiy, D. Frolovtshev, V. Firsov, P. Gostev, I. Protsenko, and M. Saygin. A spdc-based source of entangled photons and its characterization. *Journal of Russian Laser Research*, 36(6):618–629, November 2015.

[30] Paul G. Kwiat, Klaus Mattle, Harald Weinfurter, Anton Zeilinger, Alexander V. Sergienko, and Yanhua Shih. New High-Intensity Source of Polarization-Entangled Photon Pairs. *Physical Review Letters*, 75(24):4337–4341, December 1995.

[31] Baghdasar Baghdasaryan, Fabian Steinlechner, and Stephan Fritzsche. Justifying the thin-crystal ap-

proximation in spontaneous parametric down-conversion for collinear phase matching. *Physical Review A*, 103(6):063508, June 2021.

[32] Alexander Wong and Nelson Christensen. Potential multiparticle entanglement measure. *Physical Review A*, 63(4):044301, March 2001.

[33] Baiwei Mao, Yange Liu, Hongwei Zhang, Kang Yang, Ya Han, Zhi Wang, and Zhaojun Li. Complex analysis between CV modes and OAM modes in fiber systems. *Nanophotonics*, 8(2):271–285, February 2019.

[34] S. Magnitskiy, D. Frolovtshev, V. Firsov, P. Gostev, I. Protsenko, and M. Saygin. A SPDC-Based Source of Entangled Photons and its Characterization. *Journal of Russian Laser Research*, 36(6):618–629, November 2015.

[35] Xi-Lin Wang, Yi-Han Luo, He-Liang Huang, Ming-Cheng Chen, Zu-En Su, Chang Liu, Chao Chen, Wei Li, Yu-Qiang Fang, Xiao Jiang, Jun Zhang, Li Li, Nai-Le Liu, Chao-Yang Lu, and Jian-Wei Pan. 18-Qubit Entanglement with Six Photons’ Three Degrees of Freedom. *Physical Review Letters*, 120(26):260502, June 2018.

[36] Shilong Liu, Zhiyuan Zhou, Shikai Liu, Yinhai Li, Yan Li, Chen Yang, Zhaohuai Xu, Zhaodi Liu, Guangcan Guo, and Baosen Shi. Coherent manipulation of a three-dimensional maximally entangled state. *Physical Review A*, 98(6):062316, December 2018.

[37] Liang Fang, Hongya Wang, Yize Liang, Han Cao, and Jian Wang. Spin-orbit mapping of light. *Physical Review Letters*, 127(23):233901, 2021.

[38] Andrea Rubano, Filippo Cardano, Bruno Piccirillo, and Lorenzo Marrucci. Q-plate technology: a progress review [Invited]. *JOSA B*, 36(5), May 2019.

[39] Nabil Md Rakibul Hoque and Lingze Duan. A Mach-Zehnder Fabry-Perot hybrid fiber-optic interferometer operating at the thermal noise limit. *Scientific Reports*, 12(1):12130, July 2022.

[40] Long Zhu, Jiaxiong Li, Guoxuan Zhu, Lulu Wang, Chengkun Cai, Andong Wang, Shuhui Li, Ming Tang, Zuyuan He, Siyuan Yu, Cheng Du, Wenyong Luo, Jie Liu, Jiangbing Du, and Jian Wang. First demonstration of orbital angular momentum (oam) distributed raman amplifier over 18-km oam fiber with data-carrying oam multiplexing and wavelength division multiplexing. In *2018 Optical Fiber Communications Conference and Exposition (OFC)*, pages 1–3, March 2018.

[41] Sheng Zhao, Shaoqian Wang, Baoshan Gu, Congliao Yan, Sha Wang, Guoliang Deng, and Shouhuan Zhou. Controllable mode emission from all-fiber laser based on polarization rotation technology and its application in bending sensing. *Optics Communications*, 528, February 2023.

[42] Yi Li, ShuangYin Huang, Min Wang, Chenghou Tu, XiLin Wang, Yongnan Li, and HuiTian Wang. Two measurement tomography of high dimensional orbital angular momentum entanglement. *Physical Review Letters*, 130(5):050805, February 2023.